



Journal of Applied and Computational Mechanics



Research Paper

A Closed-Form Solution for Electro-Osmotic Flow in Nano-Channels

Kianoosh Rabbani^{ORCID}, Mohammad Emamzadeh^{ORCID}

Department of Mechanical and Energy Engineering, Shahid Beheshti University, Tehran, 19839 69411, Iran, Emails: k.rabbani@mail.sbu.ac.ir, M_Emamzadeh@sbu.ac.ir

Received December 21 2019; Revised April 12 2020; Accepted for publication April 12 2020.

Corresponding author: M. Emamzadeh (M_Emamzadeh@sbu.ac.ir)

© 2022 Published by Shahid Chamran University of Ahvaz

Abstract. In this article, a fluid dynamic code is implemented to investigate a non-linear model for electro-osmotic flow through a one-dimensional Nano-channel. Certain mathematical techniques are simultaneously utilized to convert the coupled system of equations into a non-linear differential correlation. This correlation is based on the mole fraction of anion. By using a modified homotopy perturbation method, the achieved non-linear differential equation is converted into a few linear differential equations. The mole fraction of anion across the channel is found by solving the linear differential equations. Finally, the distribution of the mole fraction of cation, electrical potential, and velocity are accurately derived based on the mole fraction of anion. The present study confirms that by application of a modified homotopy perturbation method, the results are in acceptable agreement with the previously validated data. However, using the proposed method here, a closed-form of the solution is achieved.

Keywords: Electro-osmotic flow, Nano-channels, numerical solution, Poisson-Nernst-Planck.

1. Introduction

Miniaturization has been one of the most rapid developments in the world of science and technology during the last century. Around 40 years ago, the concepts "micro and nano fluidics" were coined when micro-fabricated fluid systems were developed at Stanford (gas chromatography) and IBM (inkjet printer nozzles) [21]. Fluid flow through a capillary microchannel has various biotechnological applications (such as fast DNA analysis, protein separation, drug delivery systems, etc.), in solid-state and catalytic devices [1]. The flow, the electric field, and mass transfer due to the diffusion and presence of an imposed electric field between parallel plates are of great importance in electro-osmotic flow. These types of problems have been discussed in various papers (e. g. [16, 17, 18, 19]). Electro-osmotic flow (EOF) is defined as the fluid flow in a micro-/nano-sized channel or a porous medium under an imposed electric field. EOF occurs on the liquid-solid interface as a result of the spontaneous charge creation. Usually, when put in contact with water or aqueous solutions, negative charges are formed naturally on a solid surface. The positive ions in the liquid are then attracted to the negatively-charged surface, whereas the negative ions are repelled from it, forming a thin layer of net charges called the electrical double layer (EDL) [2]. In many systems, the usual balance for mass transfer is between Fick diffusion and convection of the bulk fluid [3]. This mass transfer balance is a key parameter in performance determination of an absorption heat pump [4]. Liquid pumping may also occur under a DC electric field along the outer surface of an electrode. The liquid pumping of an ionic solution is caused by the movement of mobile ions (EDL) accumulated around an electrode, and the resultant flow is the EOF. For biological applications, the ionic solution pumping mechanism needs to be better understood, which is the main concern in [5].

Field-dependent solvent polarization effects on the EDL electrostatic potential distribution and the effective EDL thickness in narrow nanofluidic confinements with thick (or overlapping) EDLs were also depicted in [6]. The effect of the size of a fluidic channel on the form of the electrostatic potential was investigated in [7]. The non-linear Poisson-Boltzmann equation was solved by using the method of matched asymptotic expansions. The electrostatic potential in a capillary filled with electrolyte was analytically derived. It was approved that by decreasing the size of the channel, the precise form of the electrostatic potential in a fluidic channel is being more important. This often occurs in microfluidic and nanofluidics applications. The results were in very good quantitative agreement with the numerical solution of the non-linear Poisson-Boltzmann equation for thin electrical double layers.

The lattice-Boltzmann method was developed in [8] to numerically simulate three-dimensional electro-osmotic flow problems in porous media. In their work, the electro-osmosis in straight cylindrical capillaries with a (non)uniform zeta-potential distribution for capillary inner radius ratios to electrical double layer thicknesses between 10 and 100 was considered.

The flow of ions through protein channels was presented in [9]. The authors focused on the numerical investigation of the effects of electrical properties of the channel on the flow. It was shown that for long channels with small permittivity (in comparison with that of the aqueous solution), the potential down the channel was significantly altered. They concluded that this potential does not satisfy a one-dimensional Poisson-Boltzmann but is a solution to a new equation.



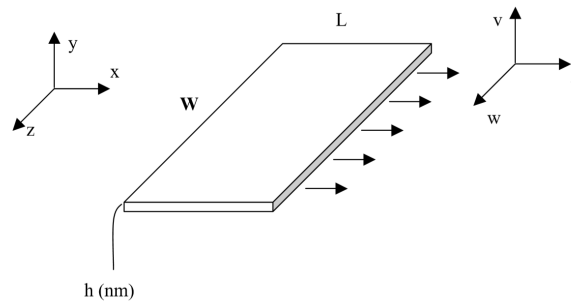


Fig. 1. One-dimensional channel geometry W "h, L "h.

A numerical model to describe the rotating EOF of the power-law fluid in a non-uniform microchannel with slip boundary condition was presented in [10]. The potential distribution of the EDL was introduced by using the non-linear Poisson-Boltzmann equation. The solution was then obtained by using finite difference method. Comparison of their results with the analytical solutions of a Newtonian fluid confirmed the validity and effectiveness of the proposed method.

A stochastic version of the Navier-Stokes equations was employed in [11] to spectrally investigate the probabilistic effects due to the influence of roughness elements and uncertainties in wall conditions due to the presence of a random distribution of nanobubble. Accordingly, a generalized mathematical expression which can be utilized as a basic scientific guideline for designing microfluidic channels was derived.

In [12], Poisson-Nernst-Planck (PNP) systems were taken into consideration in the case of vanishing permanent charge. The authors conducted a case study using simulation and singular perturbation analysis. The results for potential profiles and ion concentration profiles were given for different boundary conditions.

In [13], a solution to this problem by means of Adomian method was provided. Adomian is a powerful method to solve non-linear differential equations. In [22], EOF through nano-channels was investigated and four coupled non-linear equations were derived to calculate mole fractions of anion and cation, electrical potential, and velocity of ion flow. Zheng [22] presented an accurate solution for this problem using finite difference approach. Although the results were in acceptable agreement with experimental data, error analysis could not be done and a closed form expression for the solution was not accessible using finite difference approach.

In this paper, the non-linear system of equations introduced in Zheng [22], is converted into a non-linear ordinary differential equation system. Then the equation is solved by implementation of the homotopy perturbation method. Once the non-linear differential equation is solved, the mole fraction of anion is determined and the solution to the rest of the equations is accurately obtained.

2. Mathematical Model

A mathematical model to analyze the electro-osmotic flow in nano channels is represented here based on the research conducted in [22]. The geometry of channel is shown in Fig.1. The general three-dimensional governing equations for electro-osmotic flow are Poisson equation for the electric field, the Navier-Stokes equation for the flow field, and the mass transfer equation. First, the general three-dimensional equations are represented here. Then, assuming a dilute mixture, the mass transfer equations reduce to the PNP equations ([9, 12, 20]). The flow is assumed to be incompressible, laminar, and one-dimensional.

2.1 Poisson Equation

The Poisson equation is written in the following form:

$$\nabla^2 \varphi^*(r^*) = -\frac{1}{\epsilon_r \epsilon_0} e \sum_i z_i \rho_i(r^*) = -\frac{1}{\epsilon_r \epsilon_0} e N_A \sum_i z_i c_i(r^*) = -\frac{1}{\epsilon_r \epsilon_0} Fc \sum_i z_i X_i(r^*) \tag{1}$$

$c = \sum_i c_i + c_{solvent}$ corresponds to total molar concentration of all ions and solvent (which is supposed to be constant for each system) and $X_i = c_i / c$ denotes the mole fraction of ion species. By defining non-dimensional variables as $\varphi(r(x, y, z)) = \varphi^*(r^*) / \varphi_0$, $x = x^* / L$, $y = y^* / h$, $z = z^* / W$ the following correlation is acquired:

$$\nabla^2 \varphi = -\frac{Fch^2}{\epsilon_e \varphi_0} \sum_i z_i X_i \tag{2}$$

where $\epsilon_1 = h / L$, $\epsilon_2 = h / W$, $\epsilon_e = \epsilon_r \epsilon_0$, and $\varphi_0 = kT / e = RT / F$ (k , T , and R denote Boltzmann constant, absolute temperature in Kelvins, and universal ideal gas constant, respectively). If the volume of ions could be neglected, equation becomes:

$$\epsilon^2 \nabla^2 \varphi = -\beta \sum_i z_i X_i \tag{3}$$

$\epsilon = \lambda / h$, $\beta = c / I$, λ is the Debye length, c is the total concentration and I is the ionic strength. The boundary conditions for the equation are:

$$\begin{cases} \varphi = \varphi^0 & y = 0 \\ \varphi = \varphi^1 & y = 1 \end{cases} \tag{4}$$

2.2 Mass Transfer Equation

As the focus is on the electro-osmotic flow here, it is supposed that no externally imposed pressure gradient exists. Moreover, for nanochannels, in which there exists an externally applied pressure, as long as the pressure is not considerably large, the



pressure diffusion is neglectable compared to the electro-osmosis. In consequence, the forces which contribute in mass transfer of fluid are ordinary Fick diffusion, convection, and migration due to the presence of an electric field. At steady state, the non-dimensional mass transport equation is:

$$\nabla^2 X_i + z_i \nabla \cdot (X_i \nabla \varphi) - \text{Re.Sc} \cdot \nabla \cdot (X_i u) = 0 \tag{5}$$

where $\text{Re} = \rho U_0 h / \mu$ is the Reynolds number, $\text{Sc} = \mu / \rho D_i$ is the Schmidt number, and D_i is the diffusion coefficient. The non-dimensional velocity is defined as $u = u^* / U_0$ where U_0 is the velocity scale. For the electro-osmotic flow in micro- and nanochannels, the Reynolds number could be neglected as it is very small. Thus the non-dimensional mass transfer equation becomes:

$$\nabla \cdot (\nabla X_i + z_i X_i \nabla \varphi) = 0 \tag{6}$$

The boundary conditions are:

$$\begin{cases} X_i = X_i^0 & y = 0 \\ X_i = X_i^1 & y = 1 \end{cases} \tag{7}$$

2.3 Navier-Stokes Equation

The three-dimensional momentum equation for incompressible, steady flow is:

$$\text{Re} \cdot \vec{u} \cdot \nabla \vec{u} = -\nabla p - \frac{Fc \varphi_0 h \sum_i z_i X_i}{\mu U_0} \cdot \nabla \varphi + \nabla^2 \vec{u} \tag{8}$$

where $p = p^* / (\mu U_0 / h)$ is the dimensionless pressure. The boundary conditions (4), (7) are held for this equation too. For no-slip flow, the boundary conditions for u are $u = 0$ at the walls. As the flow is laminar (the Reynolds number is very small), the pressure driving the flow can be neglected, and x is the main direction, the Navier-Stokes equation in the x -direction could be simplified and written in the following form:

$$\varepsilon^2 \nabla^2 u = -\beta \sum_i z_i X_i \tag{9}$$

2.4 One-dimensional governing equations

For the channel shown in Fig. 1 the classical three-dimensional governing equations can be simplified. As $h \ll W$, and $h \ll L$, we have $\varepsilon_1, \varepsilon_2 \ll 1$, in the governing equations the terms with coefficients ε_1 or ε_2 are assumed to be negligible. Thus the one-dimensional governing equations can be written as:

$$\frac{d^2 \varphi}{dy^2} = -\frac{\beta}{\varepsilon^2} \sum_i X_i, \tag{10}$$

$$\frac{d^2 X_i}{dy^2} + z_i \frac{d}{dy} (X_i \frac{d\varphi}{dy}) = 0, \tag{11}$$

$$\frac{d^2 u}{dy^2} = -\frac{\beta}{\varepsilon^2} \sum_i X_i. \tag{12}$$

Comparison of Eq. (10) with Eq. (12) shows that dimensionless potential φ and velocity u are governed by the same differential equations. If the electrolyte contains monovalent cation and anion (NaCl), $z_i = 1$ and Eqs. (10) -(12) can be rewritten as:

$$\frac{d^2 \varphi}{dy^2} = -\frac{\beta}{\varepsilon^2} (X_c - X_o), \tag{13}$$

$$\frac{d}{dy} \left(\frac{dX_c}{dy} + X_c \frac{d\varphi}{dy} \right) = 0, \tag{14}$$

$$\frac{d}{dy} \left(\frac{dX_o}{dy} - X_o \frac{d\varphi}{dy} \right) = 0, \tag{15}$$

$$\frac{d^2 u}{dy^2} = -\frac{\beta}{\varepsilon^2} (X_c - X_o). \tag{16}$$

where X_o and X_c are mole fractions of anion and cation respectively. Boundary conditions of Eqs. (13) -(16) are given in the following form:

$$\begin{cases} \varphi(0) = \varphi_0, \varphi(1) = \varphi_1, X_o(0) = X_o(1) = X_o^0, \\ u(0) = u(1) = 0, X_c(0) = X_c(1) = X_c^0. \end{cases} \tag{17}$$

For a real microchannel or nanochannel, if the inner surfaces of the channel are fabricated at the same environment and at the same time, the electrochemical properties of different surfaces will be equal. Therefore, the channel is symmetric. For symmetrical channels, $\varphi_0 = \varphi_1 = 0$ [22]. The above system of differential equations with boundary conditions has been numerically solved in [22]. However, in this paper, in order to decrease the amount of computations, the system of equations is converted to one non-linear differential equation based on the mole fraction of anion. Other variables are found from the mole fraction of anion.



3. Converting The System of Differential Equations to an Ordinary Differential Equation

Since Eqs. (13) and (16) are equivalent with the same boundary conditions, solving Eqs. (13) -(15) gives:

$$\varphi(1) - \varphi(0) = a \int_0^1 \frac{dy}{X_c} - \ln \left(\frac{X_c(1)}{X_c(0)} \right), \quad \varphi(1) - \varphi(0) = b \int_0^1 \frac{dy}{X_o} + \ln \left(\frac{X_o(1)}{X_o(0)} \right). \quad (18)$$

By substitution of boundary condition of Eq. (17) into Eq. (18), $a = b = 0$ is obtained. Therefore, Eqs. (14) and (15) are modified as:

$$\int_0^y d\varphi = - \int_{X_c^0}^{X_c} \frac{dX_c}{X_c}, \quad \int_0^y d\varphi = \int_{X_o^0}^{X_o} \frac{dX_o}{X_o} \quad (19)$$

resulting in

$$\varphi(y) = - \ln \left(\frac{X_c}{X_c^0} \right), \quad \varphi(y) = \ln \left(\frac{X_o}{X_o^0} \right) \quad (20)$$

Since $\ln(X_o / X_o^0) = - \ln(X_c / X_c^0)$ then

$$X_c(y) \cdot X_o(y) = X_c^0 \cdot X_o^0 \quad (21)$$

By differentiating Eq. (20) with respect to y , substituting the results into Eq. (13) and employing Eq. (21), a non-linear differential equation is derived:

$$\begin{cases} X_o \frac{d^2 X_o}{dy^2} - \left(\frac{dX_o}{dy} \right)^2 + \frac{X_c^0 X_o^0 \beta}{\varepsilon^2} X_o - \frac{\beta}{\varepsilon^2} X_o^3 = 0, \\ X_o(0) = X_o(1) = X_o^0. \end{cases} \quad (22)$$

where the boundary conditions are as follows:

$$\begin{cases} \varepsilon = 0.04, \beta = 188.679, \\ X_o(0) = X_o(1) = X_o^0 = 0.00254 \\ X_c(0) = X_c(1) = X_c^0 = 0.00276 \end{cases} \quad (23)$$

In order to solve Eq. (22), the non-linear equation is divided to certain linear differential equations by applying the new homotopy method introduced in [15].

4. Semi- Analytic Approach to Solve Eq. (22)

In this section, an effective method which is introduced in [14] is applied to solve the non-linear problem. Certain improvements have been conducted to enhance the accuracy of this method [15]. In these kinds of methods, a non-linear problem is converted to certain simple linear or non-linear problems. Thus, the final solution to the non-linear problem can be introduced as a series form of the solutions to the easier problems. Here, the non-linear problem with the below boundary conditions is considered:

$$\begin{cases} N(X_o(y)) - f(y) = 0, \quad y \in \Omega \\ B(x, \frac{\partial x}{\partial n}) = 0, \quad n \in \Gamma, \end{cases} \quad (24)$$

where N and B are general differential and boundary operators respectively and f is a known analytic function. According to Eq. (22), $f(y) = 0$. Thus, based on Eq. (24) and using the concepts defined in [15], a homotopy perturbation is defined as below:

$$H(\psi, p) = (N(\psi)) + (p - 1)(N(X_o)) = 0, \quad p \in [0, 1] \quad (25)$$

and

$$X_o(y) \simeq \psi(y) = \psi_0(y) + p \psi_1(y) + p^2 \psi_2(y) + p^3 \psi_3(y) + \dots \quad (26)$$

where p is an embedding parameter and X_o is an initial guess for $X_o(y)$. Since p varies between 0 and 1, $N(\psi)$ changes between $N(X_o)$ and 0. The solution of Eq. (24) for $p = 1$ and $X_o(y) \simeq \lim_{p \rightarrow 1} \psi(y)$ is obtained. From boundary condition (23) and using Eq. (26):

$$\begin{cases} \psi_0(0) = X_o(0) = 0.00254, \text{ and } \psi_i(0) = 0, \quad i = 1, 2, 3, \dots \\ \psi_0(1) = X_o(1) = 0.00254, \text{ and } \psi_i(1) = 0, \quad i = 1, 2, 3, \dots \end{cases} \quad (27)$$

Thus, an initial guess can be written as follows:

$$\psi_0(y) = X_o(y) = 0.00254 \quad (28)$$

Therefore, considering Eqs. (22) and (25), the non-linear operator N is given by:



$$N(X_o) = X_o \frac{d^2 X_o}{dy^2} - \left(\frac{dX_o}{dy}\right)^2 + \eta X_o - \delta X_o^3 \tag{29}$$

where $\eta = X_c^0 X_o^0 \beta / \varepsilon^2 = 0.8266498688$, $\delta = \beta / \varepsilon^2 = 1.179243750 \times 10^5$. Substituting Eqs. (26) and (27) in Eq. (25) gives:

$$\left\{ \begin{aligned} & \left(\sum_{i=0}^{\infty} p^i \psi_i(y) \right) \frac{d^2 \left(\sum_{i=0}^{\infty} p^i \psi_i(y) \right)}{dy^2} - \left(\frac{d \left(\sum_{i=0}^{\infty} p^i \psi_i(y) \right)}{dy} \right)^2 + \eta \sum_{i=0}^{\infty} p^i \psi_i(y) - \delta \left(\sum_{i=0}^{\infty} p^i \psi_i(y) \right)^3 \\ & + (p-1) \left(X_o(y) \right) \frac{d^2 X_o(y)}{dy^2} - \left(\frac{dX_o(y)}{dy} \right)^2 + \eta X_o(y) - \delta \left(X_o(y) \right)^3 = 0. \end{aligned} \right. \tag{30}$$

With rearrangement of Eq. (30) in terms of p powers and using Eq. (25), it is concluded that the coefficients of p powers are equal to zero. Thus Eq. (22) is converted to the below differential equations:

$$\{ \psi_0(y) = X_o(y) = 0.00254. \tag{31}$$

$$\left\{ \begin{aligned} & \psi_1''(y) \psi_0(y) - (\psi_1'(y))^2 + \eta \psi_0(y) - 2\psi_0'(y) \psi_1'(y) + \psi_0''(y) \psi_0(y) + \eta \psi_1(y) \\ & - 3\delta(\psi_0(y))^2 \psi_1(y) - \delta(\psi_0(y))^3 + \psi_0''(y) \psi_1(y) = 0, \\ & \psi_1(0) = \psi_1(1) = 0. \end{aligned} \right. \tag{32}$$

$$\left\{ \begin{aligned} & \psi_2''(y) \psi_0(y) - (\psi_2'(y))^2 + \eta \psi_2(y) - 2\psi_0'(y) \psi_2'(y) - 3\delta(\psi_0(y))^2 \psi_2(y) \\ & + \psi_1''(y) \psi_1(y) - 3\delta \psi_0(y) (\psi_1(y))^2 + \psi_0''(y) \psi_2(y) = 0, \\ & \psi_2(0) = \psi_2(1) = 0. \end{aligned} \right. \tag{33}$$

$$\left\{ \begin{aligned} & \psi_3''(y) \psi_0(y) + (\psi_3''(y)) \psi_3(y) - 2\psi_0'(y) \psi_3'(y) - 6\delta \psi_0(y) \psi_1(y) \psi_2(y) + \eta \psi_3(y) \\ & - 3\delta(\psi_0(y))^2 \psi_3(y) + \psi_1''(y) \psi_2(y) - \delta(\psi_1(y))^3 + \psi_2''(y) \psi_1(y) \\ & - 2\psi_1'(y) \psi_2'(y) = 0, \\ & \psi_3(0) = \psi_3(1) = 0. \end{aligned} \right. \tag{34}$$

By substitution of Eq. (31) in Eq. (32), the solution of differential Eq. (32) is found as:

$$\psi_1(y) = -4.604873974 \times 10^{-15} e^{23.94015525y} + 1.148933969 \times 10^{-4} (1 - e^{-23.94015525y}) \tag{35}$$

Substituting Eqs. (31) and (35) in Eq. (33) leads to a simple differential equation in terms of ψ_2 function, which can be solved easily:

$$\begin{aligned} \psi_2(y) = & 7.887750425 \times 10^{-7} e^{23.94015525y} + 19680.24413e^{-23.94015525y} + 4.362999428 \times 10^{-27} e^{47.8803105y} \\ & - 0.8148188226 \times 10^{-5} e^{-47.88031050y} (e^{47.88031050y} + 0.9680373359 \times 10^{-1} e^{71.82046575y} \\ & - 0.3333333331 + 2.415290808 \times 10^9 e^{23.94015525y}) \end{aligned} \tag{36}$$

Similarly, the solution to Eq. (34) is found as:

$$\psi_3(y) = -1.391981968 \times 10^{-17} e^{23.94015525y} - 3.473049157 \times 10^{-7} (1 - e^{-23.94015525y}) \tag{37}$$

To obtain a solution of Eq. (22) with acceptable accuracy, the four first terms of series (26) are taken into consideration. More terms of the summation could be considered if higher accuracy is required.

$$X_o(y) \simeq \sum_{i=0}^3 \psi_i(y) = 0.00264709 + 2.71606 \times 10^{-6} e^{-47.8803y} - 0.000114112e^{-23.9402y} - 2.57088 \times 10^{-15} e^{23.9402y} + 4.363 \times 10^{-27} e^{47.8803y} \tag{38}$$

In order to evaluate the error of the presented method, the above solution is substituted in the equation of mole fraction of anion distribution (Eq. (22)). The corresponding results are given in table.1.

Table 1. Absolute errors for $X_o(y)$.

y (dimensionless)	Absolute errors
0.0	7.2e-6
0.1	5.1e-7
0.2	1.5e-6
0.3	1.6e-6
0.4	1.6e-6
0.5	1.6e-6
0.6	1.6e-6
0.7	1.6e-6
0.8	1.5e-6
0.9	5.1e-7
1.0	7.2e-6



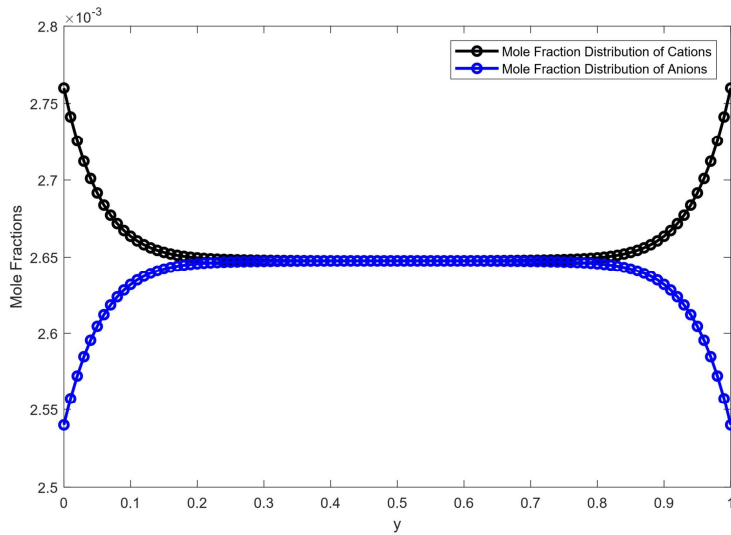


Fig. 2. The mole fraction distribution of cations and anions across the channel.

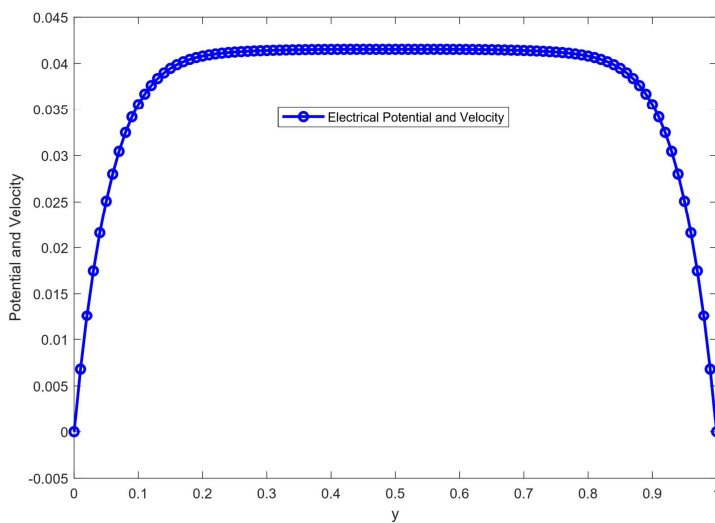


Fig. 3. The potential and velocity profile across the channel.

Substituting Eq. (38) in Eq. (21) and applying the boundary conditions (23), mole fraction of cation distribution is found in the following form:

$$X_c(y) \approx (7.0104 \times 10^{-6})(0.00264709 + 2.71606 \times 10^{-6} e^{-47.8803y} - 0.000114112 e^{-23.9402y} - 2.57088 \times 10^{-15} e^{23.9402y} + 4.363 \times 10^{-27} e^{47.8803y})^{-1} \quad (39)$$

In Fig. 2, the mole fraction distribution of cations and anions across the channel is shown. Both mole fractions and y are non-dimensional. As it is clear from Fig.2, the mole fraction of cations increases while the distance to the wall decreases. However, the mole fraction of anions decreases as the distance to the wall decreases: the increment of the cation concentration equals the decrement of the anion concentration. The concentration difference between cation and anion species reaches its maximum at the wall. In the bulk of the channel, cations and anions mole fractions are the same (difference between $X_o(y)$ and $X_c(y)$ for $y = 0.5$ is equal to 2×10^{-6} and this value is similar to the results given in [22]), confirming that the electrolytic solution is neutral in the bulk.

The values of sodium mole fraction $X_c(y)$ and chloride mole fraction $X_o(y)$ according to Eqs. (39) and (38) are given in table 2. Also, the results obtained from a code which is developed based on the finite difference approach in [22] are presented here.

Table 2. Values of cation and anion distribution.

y (dimensionless)	$X_c(y)$	$X_c(y)$ form [22]	$X_o(y)$	$X_o(y)$ from [22]
0.0	0.00276	0.00276	0.00254	0.00254
0.1	0.00265692	0.0026571803	0.00263855	0.0026383916
0.2	0.00264932	0.0026485279	0.00264612	0.0026469254
0.3	0.00264877	0.0026477585	0.00264666	0.0026476253
0.4	0.00264874	0.0026476733	0.00264669	0.0026476661
0.5	0.00264874	0.0026476606	0.0026467	0.0026476635
0.6	0.00264874	.0026476733	0.00264669	0.0026476661
0.7	0.00264877	0.002647758	0.00264666	0.0026476253
0.8	0.00264932	0.0026485279	0.00264612	0.0026469254
0.9	0.00265692	0.0026571803	0.00263855	0.0026383916
1.0	0.00276	0.00276	0.00254	0.00254



Using Eqs. (20) and (38) the solution of electrical potential and velocity are found as:

$$\varphi(y) = \ln\left(\frac{X_o}{X_o^0}\right) = \ln\left(\frac{1}{0.00254} (0.00264709 + 2.71606 \times 10^{-6} e^{-47.8803y} - 0.000114112e^{-23.9402y} - 2.57088 \times 10^{-15} e^{23.9402y} + 4.363 \times 10^{-27} e^{47.8803y})\right) \quad (40)$$

Since Eqs. (13) and (16) are equal, $\varphi(y) = u(y)$. The solution of electrical potential and velocity are shown in Fig. 3.

5. Conclusion

The coupled non-linear system of equations (Eqs. (13)-(16)) was solved in [22]. However, in this paper, the above system was converted to a non-linear differential equation. In this research, the non-linear differential equation governing the fluid flow in Nano-channels was solved by the proposed method. A comparison of our results with those found from previous methods available in the literature demonstrates the simplicity and effectiveness of the proposed method. It was also demonstrated that our results are in acceptable agreement with previously validated data. Furthermore, error analysis, which could be done by substituting the closed-form of the solution in the equations, guarantees the validity of our results. The numerical error analysis shows that the fluid dynamic code accurately solves the governing equations.

Author Contributions

M. Emamzadeh planned the scheme, initiated the research work, and suggested the possible innovations; K. Rabbani resumed the research about the previous similar works, developed the mathematical modeling, and planned the numerical method to solve the problem. All authors discussed the results, reviewed, and approved the final version of the manuscript.

Acknowledgments

Not applicable.

Conflict of Interest

The authors declared no potential conflicts of interest with respect to the research, authorship, and publication of this article.

Funding

The authors received no financial support for the research, authorship, and publication of this article.

Data Availability Statements

The datasets generated and/or analyzed during the current study are available from the corresponding author on reasonable request.

Nomenclature

φ^*	Electrical potential [Volts]	Z_i	Valence of ion species
r^*	Vector of location in Cartesian coordinates [m]	ρ_i	Density of electrolyte i [kg/m ³]
ϵ_r	Dielectric constant of the substance [F/m]	N_A	Avogadro number
ϵ_0	Permittivity of free space [F/m]	F	Faraday's constant [C/mol]
e	Elementary charge [C]		

References

- [1] Huang, G., Willems, K., Soskine, M., Wloka, C., Maglia, G., Electro-osmotic capture and ionic discrimination of peptide and protein biomarkers with FraC nanopores, *Nat Commun*, 8, 935, 2017.
- [2] Lim, C., Lim, A. & Lam, Y., Ionic Origin of Electro-osmotic Flow Hysteresis, *Sci Rep*, 6, 22329, 2016.
- [3] Conlisk, A. T., Falling Film Absorption on a Cylindrical Tube, *AIChE J*, 38(11), 1992, 1716-1728.
- [4] Conlisk, A. T., Analytical Solutions for the Heat and Mass Transfer in a Falling Film Absorber, *Chem Eng Sci*, 50(4), 1995, 651-660.
- [5] Hwal Shin, J., Hwee Kim, G., Kim, I. et al., Ionic liquid flow along the carbon nanotube with DC electric field, *Sci Rep*, 5, 11799, 2015.
- [6] Das, S., Chakraborty, S., Mitra, S. K., Redefining electrical double layer thickness in narrow confinements: Effect of solvent polarization, *Physical Review E*, 85(5), 2012, 051508.
- [7] Dimiter, N. P., Gabriel, P. L., Electrostatic potential and electroosmotic flow in a cylindrical capillary filled with symmetric electrolyte: Analytic solutions in thin double layer approximation, *Journal of Colloid and Interface Science*, 294(2), 2006, 492-498.
- [8] Hlushkou, D., Kandhai, D., Tallarek, U., Coupled lattice-Boltzmann and finite-difference simulation of electroosmosis in microfluidic channels, *Int J Numer Meth Fluids*, 46(5), 2004, 507-532.
- [9] Barcion, V., Chen, D. P., Eisenberg, R. S., Ion Flow Through Narrow Membrane Channels, *SIAM Journal on Applied Mathematics*, 52(5), 1992, 1405-1425.
- [10] Wang, S., Li, N., Zhao, M., Azese, M. N., Effect of Slip Velocity on the Rotating Electro-Osmotic Flow of the Power-Law Fluid in a Slowly Varying Microchannel, *Z Naturforsch*, 73(9), 2018, 825-831.
- [11] Chakraborty, S., Towards a generalized representation of surface effects on pressure-driven liquid flow in microchannels, *Applied Physics Letters*, 90(3), 2007, 034108.
- [12] Barcion, V., Chen, D.P., Eisenberg, R. S., Jerome, J. W., Qualitative Properties of Steady-State Poisson- Nernst-Planck Systems: Perturbation and Simulation Study, *SIAM Journal on Applied Mathematics*, 57(3), 1997, 631-648.
- [13] Glayeri, A., Rabbani, M., Computation Adomian Method for Solving Non-linear Differential Equation in the Fluid Dynamic, *International Journal of Mechatronics, Electrical and Computer Technology*, 5(14), 2015, 122-126.
- [14] He, Ji.H., A coupling method of a homotopy technique and a perturbation technique for non-linear problems, *International Journal of Non-linear Mechanics*, 35(1), 2000, 37-43.
- [15] Rabbani, M., New Homotopy Perturbation Method to Solve Non-Linear Problems, *J Math Comput Sci*, 7(4), 2013, 272-275.
- [16] Bockris, J. O'M., Reddy, A. K. N., *Modern Electrochemistry*, Vol. 1: Ionics, Second Edition, Plenum Press, New York and London, 1998.



- [17] Delahay, P., *Double Layer and Electrode Kinetics*, Wiley Interscience, New York ,1965.
[18] Hunter, R. J., *Zeta Potential in Colloid Science*, Academic Press: London, 1981.
[19] Newman, J. S, *Electrochemical Systems*, Prentiss-Hall : Englewood Cliffs, NJ, 1973.
[20] Robinson, R. A., Stokes, R. H, *Electrolyte Solutions*, Academic Press: New York, 1959.
[21] Kulinsky, L., *Study of the fluid flow in micro fabricated microchannels*, UMI Dissertation Service, University of California, Berkeley, 1998.
[22] Zheng, Z., *Electrokinetic Flow in Micro- and Nano-Fluidic Components*, Ph.D. Thesis, Ohio State University, Ohio State, 2003.

ORCID iD

Kianoosh Rabbani  <https://orcid.org/0000-0002-9479-0925>

Mohammad Emamzadeh  <https://orcid.org/0000-0003-3385-1269>



© 2022 Shahid Chamran University of Ahvaz, Ahvaz, Iran. This article is an open access article distributed under the terms and conditions of the Creative Commons Attribution-NonCommercial 4.0 International (CC BY-NC 4.0 license) (<http://creativecommons.org/licenses/by-nc/4.0/>).

How to cite this article: Rabbani K., Emamzadeh M. A Closed-Form Solution for Electro-Osmotic Flow in Nano-Channels, *J. Appl. Comput. Mech.*, 8(2), 2022, 510–517. <https://doi.org/10.22055/JACM.2020.32020.1952>

Publisher's Note Shahid Chamran University of Ahvaz remains neutral with regard to jurisdictional claims in published maps and institutional affiliations.

